Journal of Systems Engineering and Electronics
Vol. 34, No. 1, February 2023, pp.149 – 159

Hybrid TDOA/FDOA and track optimization of UAV swarm based on A-optimality

LI Hao, SUN Hemin, ZHOU Ronghua*, and ZHANG Huainian
Department of Intelligence, Air Force Early Warning Academy, Wuhan 430019, China

Abstract: The source location based on the hybrid time difference of arrival (TDOA)/frequency difference of arrival (FDOA) is a basic problem in wireless sensor networks, and the layout of sensors in the hybrid TDOA/FDOA positioning will greatly affect the accuracy of positioning. Using unmanned aerial vehicle (UAV) as base stations, by optimizing the trajectory of the UAV swarm, an optimal positioning configuration is formed to improve the accuracy of the target position and velocity estimation. In this paper, a hybrid TDOA/FDOA positioning model is first established, and the positioning accuracy of the hybrid TDOA/FDOA under different positioning configurations and different measurement errors is simulated by the geometric dilution of precision (GDOP) factor. Second, the Cramer-Rao lower bound (CRLB) matrix of hybrid TDOA/FDOA location under different moving states of the target is derived theoretically, the objective function of the track optimization is obtained, and the track of the UAV swarm is optimized in real time. The simulation results show that the track optimization effectively improves the accuracy of the target position and velocity estimation.

Keywords: unmanned aerial vehicle (UAV) swarm, time difference of arrival (TDOA), frequency difference of arrival (FDOA), A-optimality, track optimization.

DOI: 10.23919/JSEE.2023.000008

1. Introduction

The U.S. Department of Defense pointed out in the "Unmanned Aerial Vehicle (UAV) System Roadmap 2005–2030" that by 2025, UAV swarm will have battlefield cognitive ability and can fully self-organizing operations [1]. UAV has been widely used in national defense construction and civil field. With the in-depth research of UAV technology, UAV autonomous swarm system can complete various complex and changeable tasks through close cooperation, and has excellent coordination, intelligence and autonomy, which has become an important direction of UAV research. UAV swarm operation refers to the process in which a group of UAVs with partial autonomous capability complete combat tasks under the monitoring of combat command system through relevant auxiliary operations [2,3].

Since the Middle East War and the Gulf War, the development of UAV swarm has received much attention from countries all over the world, and has had a revolutionary impact on the field of intelligence surveillance and reconnaissance. In the 21st century, the miniaturization, intelligence and information fusion of avionics equipment, as well as the improvement of loading capacity, make it possible for UAV to load passive positioning equipment. The UAV intercepts the signal of the target radiation source and performs passive positioning. The mode of positioning and then implementing the strike is realistic and feasible [4]. Compared with the use of space-borne platforms for positioning, the advantages of using UAV swarm for passive positioning are mainly [5,6]:

(i) High positioning accuracy. Since the flying altitude of the UAV is much lower than that of the reconnaissance satellite, the ground target signal received by reconnaissance is stronger, and the accuracy of parameter measurement is higher, thereby improving the positioning accuracy.

(ii) Flexible station layout. Reconnaissance satellites can only fly in accordance with a predetermined orbit, while UAV swarm can select flight areas or optimize trajectories according to the intention of the ground measurement and control station, so as to realize real-time

Manuscript received December 29, 2020.
*Corresponding author.
This work was supported by the National Natural Science Foundation of China (61502522), Equipment Pre-Research Field Fund (JZX7Y20190253036101), Equipment Pre-Research Ministry of Education Joint Fund (6141A02033703), and Hubei Provincial Natural Science Foundation (2019CFC897).

reconnaissance and positioning of key areas or key targets.

(iii) Low cost and low combat loss. The cost of manufacturing and launching UAV swarm is much lower than that of reconnaissance satellites, which has economic advantages; and the swarm is unmanned, so there is no need to consider casualties in operations.

The current passive positioning system is mainly divided into angle of arrival (AOA) [7,8], received signal strength (RSS)[9,10], time difference of arrival (TDOA) [10,11], frequency difference of arrival (FDOA) [12,13] and the combination of the above positioning systems. In the actual battlefield environment, different positioning systems have different error statistics characteristics and corresponding performance. There is no single positioning system that can show the best performance in all channels and network environments on the battlefield. Compared with the single positioning system, the hybrid positioning system has the advantages of high target observation reliability, fewer sensors required under the same positioning accuracy, high system reliability and strong system survivability [14]. In the hybrid positioning system, the hybrid TDOA/FDOA positioning combines the advantages of a single TDOA positioning and a single FDOA positioning, and has been widely used. According to the motion state of the sensor and the target, the hybrid TDOA/FDOA positioning can be divided into three types: the positioning and velocity estimation of the moving target by the stationary sensor, the positioning of the stationary target by the motion sensor, and the positioning and velocity estimation of the moving target by the motion sensor [15]. For the application of UAV swarm to target positioning, usually only the latter two cases are considered.

The main factors that affect the accuracy of hybrid TDOA/FDOA positioning and velocity estimation are the baseline length of the deployment station, measurement error and site error [16], among which the deployment method of the sensor will greatly affect the final positioning accuracy. Therefore, according to the motion state of the target, real-time planning of the UAV's track to achieve a reasonable deployment of stations is extremely important for improving the accuracy of target positioning and velocity estimation. Quo et al. [17] used the signal strength of the target radiation source to control the movement of the UAV, and Liu et al. [18] controlled the velocity and direction of the UAV with the position of precision factor as the criterion. Kim et al. [19] studied the impact of sensor linear motion on positioning accuracy, and analyzed the geometric dilution of precision (GDOP) in a fixed configuration with TDOA/FDOA sensors mounted on UAV swarm flying in different velocity directions. Takabayashi et al. [20] preliminarily studied the trajectory planning method when only one base station is moving in the TDOA positioning process. In [21], James et al. used the minimum Cramer-Rao lower bound (CRLB) as a performance index to study the optimal track of the observer to minimize the current target position error, target velocity error, and predicted target position error.

Frew et al. [22] adopted the optimization principle of minimum positioning covariance, and gave a "Z"-shaped maneuver mode. Semper et al. [23] proposed that the optimization function based on the minimum trace of the filter covariance matrix is relatively simple and the amount of calculation is relatively small. Cao [24] optimized the attack track of anti-radiation UAV in a single step in. Moreno-salinas et al. [25] took maximizing the lower bound of the Fisher information array as the performance index, and solved the optimal track of fixed targets and uniformly moving targets in the case of two-dimensional (2-D) angle measurement only.

In practical applications, the UAV swarm is affected by its own motion constraints and cannot achieve the optimal configuration for target positioning in a short time [26]. Therefore, how to optimize the track of the UAV swarm and constantly change the relative configuration with the target is crucial [27]. In this paper, the minimum trace value of the CRLB matrix is used as the optimization function, and the track optimization of the UAV swarm platform equipped with the TDOA/FDOA sensor is analyzed emphatically. Based on A-optimality criterion, the real-time single step optimization of UAV swarm track is carried out [28,29].

2. Hybrid TDOA/FDOA positional model

As shown in Fig. 1, in a 2-D scenario, the UAV swarm hybrid TDOA/FDOA positioning is to obtain the position and velocity of the target radiation by receiving TDOA information and FDOA information between two independent receivers. Assume that the position and velocity of the target radiation source to be estimated are $\boldsymbol{u}=[x,y]^{\mathrm{T}}$ and $\dot{\boldsymbol{u}}=[\dot{x},\dot{y}]^{\mathrm{T}}$, respectively, and the position and velocity of each UAV base station are $\boldsymbol{s}_i=[x_i,y_i]^{\mathrm{T}}$ and $\dot{\boldsymbol{u}}=[\dot{x},\dot{y}]^{\mathrm{T}}$ ($i=1,2,\cdots,M$), where T represents the transposition of the matrix. At least three receiving base stations are required in a 2-D scenario to determine the position and velocity of the target radiation source [15]. This paper studies the hybrid TDOA/FDOA positioning

of $M = 4$ receiving base stations, which can utilize redundant information to improve the accuracy of positioning.

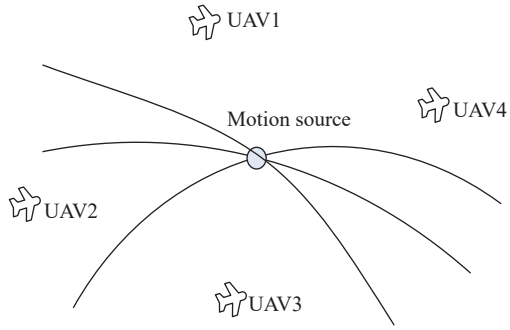

Fig. 1 Location diagram

Without loss of generality, suppose the first UAV base station is used as the reference base station, and the distance between the radiation source $\boldsymbol{u}$ and the base station $\boldsymbol{s}_i$ is

$$d_i = \|\boldsymbol{s}_i - \boldsymbol{u}\|_2, \quad i = 1, 2, \cdots, M \tag{1}$$

where $\|\cdot\|_2$ means finding the norm of 2. Then the distance difference between the target source reaching the reference base station and reaching other base stations is

$$d_{i1} = \mathrm{c}\tau_{i1} = d_i - d_1 \tag{2}$$

where c represents the velocity of light, and τ_{i1} represents the time difference between the radiation source reaching the reference base station and other base stations, that is, TDOA. Substituting (1) into (2), the shift term can be obtained as

$$\begin{aligned} &d_{i1}^2 + 2d_{i1}d_1 = d_i^2 - d_1^2 = \\ &(\boldsymbol{s}_i - \boldsymbol{u})^{\mathrm{T}}(\boldsymbol{s}_i - \boldsymbol{u}) - (\boldsymbol{s}_1 - \boldsymbol{u})^{\mathrm{T}}(\boldsymbol{s}_1 - \boldsymbol{u}) = \\ &\boldsymbol{s}_i^{\mathrm{T}}\boldsymbol{s}_i - \boldsymbol{s}_1^{\mathrm{T}}\boldsymbol{s}_1 - 2(\boldsymbol{s}_i - \boldsymbol{s}_1)^{\mathrm{T}}\boldsymbol{u}, \quad i = 2, \cdots, M. \end{aligned} \tag{3}$$

It can be seen from (3) that this equation is a nonlinear equation about the position of the radiation source, which does not contain the velocity information of the radiation source. Therefore, the TDOA positioning can only obtain the position of the radiation source. After introducing the Doppler rate of change, the instantaneous velocity of the radiation source can be solved, and the positioning accuracy can also be improved. In order to make effective use of FDOAs, calculate the derivative of time to get the distance change rate from (1).

$$\dot{d}_i = \frac{(\dot{\boldsymbol{u}} - \dot{\boldsymbol{s}}_i)^{\mathrm{T}}(\boldsymbol{u} - \boldsymbol{s}_i)}{d_i} \tag{4}$$

Then the change rate of the distance difference between the radiant source reaching the ith base station and the reference base station is

$$\dot{d}_{i1} = \dot{d}_i - \dot{d}_1. \tag{5}$$

Therefore, the time differential of (3) is

$$\begin{aligned} &2\left(\dot{d}_{i1}d_{i1} + d_{i1}d_1 + d_{i1}\dot{d}_1\right) = \\ &2\left(\dot{\boldsymbol{s}}_i^{\mathrm{T}}\dot{\boldsymbol{s}}_i^{\mathrm{T}} - \dot{\boldsymbol{s}}_1^{\mathrm{T}}\dot{\boldsymbol{s}}_1 - (\dot{\boldsymbol{s}}_i - \dot{\boldsymbol{s}}_1)^{\mathrm{T}}\boldsymbol{u} - (\dot{\boldsymbol{s}}_i - \dot{\boldsymbol{s}}_1)^{\mathrm{T}}\dot{\boldsymbol{u}}\right) \end{aligned} \tag{6}$$

where $i = 2, 3, \cdots, M$. Equation (5) is a nonlinear equation group composed of TDOA and FDOA, which contains the position and velocity information of the radiation source.

Note that $\boldsymbol{d} = [d_{21}, d_{31}, \cdots, d_{M1}]^{\mathrm{T}}$ is the distance difference including the measurement noise, $\dot{\boldsymbol{d}} = \left[\dot{d}_{21}, \dot{d}_{31}, \cdots, \dot{d}_{M1}\right]^{\mathrm{T}}$ is the change rate of the distance difference including the measurement noise. Correspondingly, $\boldsymbol{d}^0 = [d_{21}^0, d_{31}^0, \cdots, d_{M1}^0]^{\mathrm{T}}$ is the true value of the distance difference, and $\dot{\boldsymbol{d}}^0 = \left[\dot{d}_{21}^0, \dot{d}_{31}^0, \cdots, \dot{d}_{M1}^0\right]^{\mathrm{T}}$ is the true value of the distance difference. Therefore, the TDOA/FDOA positioning equation is obtained as

$$\boldsymbol{d} = \mathrm{c}\boldsymbol{\tau} = \boldsymbol{d}^0 + \boldsymbol{n}, \tag{7}$$

$$\boldsymbol{F}_d = \frac{f_0}{\mathrm{c}}\left(\dot{\boldsymbol{d}}^0 + \dot{\boldsymbol{n}}\right), \tag{8}$$

where $\boldsymbol{N}_\tau = [n_{21}, n_{31}, \cdots, n_{M1}]^{\mathrm{T}}$ and $\dot{\boldsymbol{N}}_f = [\dot{n}_{21}, \dot{n}_{31}, \cdots, \dot{n}_{M1}]^{\mathrm{T}}$ are the corresponding measurement noises respectively; $\boldsymbol{\tau} = [\tau_{21}, \tau_{31}, \cdots, \tau_{M1}]^{\mathrm{T}}$ is TDOA, $\boldsymbol{F}_d = [f_{d21}, f_{d31}, \cdots, f_{dM1}]^{\mathrm{T}}$ is FDOA; f_0 is the frequency of the radiation source, the two sets of noise variables are independently distributed and the mean value is zero.

3. Positioning accuracy analysis

The positioning accuracy is usually measured by GDOP. The smaller the GDOP value, the higher the positioning accuracy. According to the definition of GDOP, we have

$$\mathrm{GDOP}^2 = \mathrm{tr}\left\{\mathrm{E}\left(\Delta\boldsymbol{r}\Delta\boldsymbol{r}^{\mathrm{T}}\right)\right\} \tag{9}$$

where, $\Delta\boldsymbol{r}$ is the positioning error term [30].

Typical station layout methods are square, Y-shaped, T-shaped, and diamond. Factors such as the length of the baseline, measurement errors, and station site errors also affect the positioning accuracy. To improve the positioning accuracy of the target, it is the key to choose the optimal station layout plan. The following is an analysis of the four typical GDOP deployment methods.

After simulation, the positioning error distribution diagrams as shown in Fig. 2−Fig. 4 are obtained. The analysis shows that the greater the measurement error, the greater the positioning error; when the square cloth is stationed, and the target is in the diagonal direction of the X-axis and Y-axis, the accuracy is better than other directions; when the station is Y-shaped, the positioning error is more evenly distributed; when the station is T-shaped, the positioning error in the positive direction of the Y-axis is larger, and the positioning accuracy in the X-axis direction is higher; when the diamond is stationed, the positioning accuracy in the X-axis and Y-axis directions is higher than other directions.

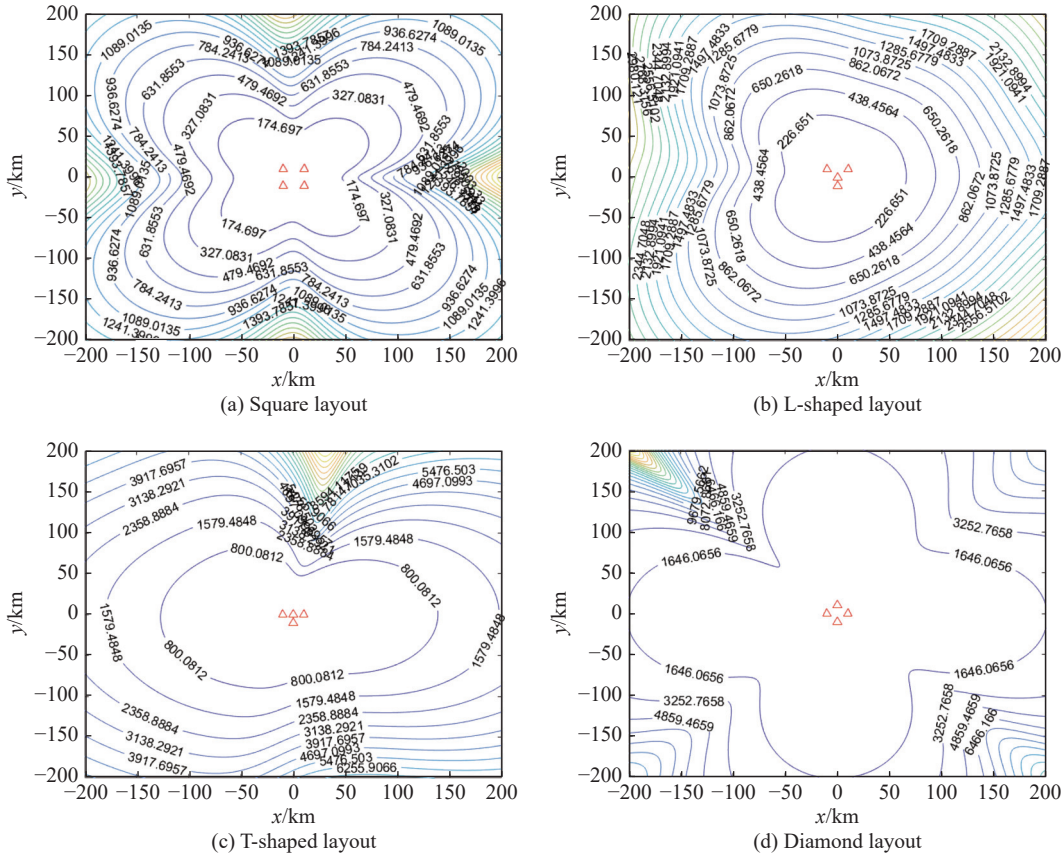

Fig. 2 5 ns/5 Hz positioning error

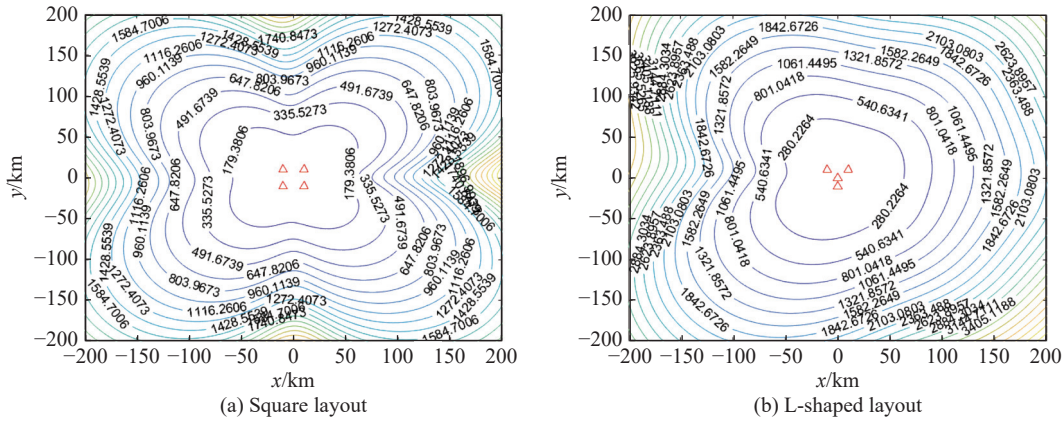

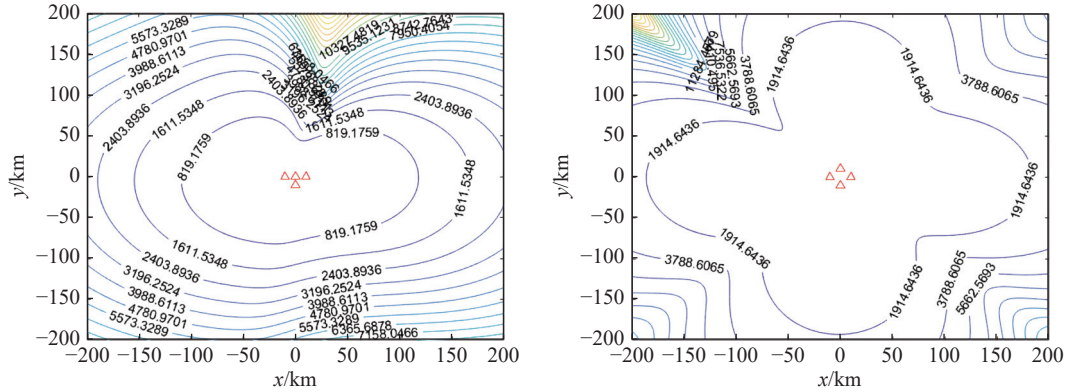

(c) T-shaped layout (d) Diamond layout

Fig. 3 10 ns/5 Hz positioning error

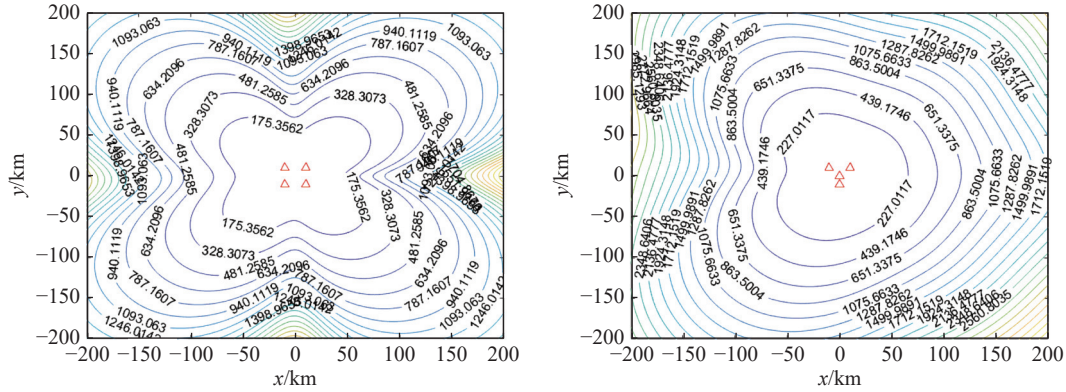

(a) Square layout (b) L-shaped layout

(c) T-shaped layout (d) Diamond layout

Fig. 4 5 ns/10 Hz positioning error

4. Track optimization

4.1 A-optimality criteria

From (7) and (8), the observation vector composed of TDOA and FDOA [31] can be obtained as

$$\boldsymbol{Y}_\tau = [\tau_{21}, \tau_{31}, \cdots, \tau_{M1}]^{\mathrm{T}}, \tag{10}$$

$$\boldsymbol{Y}_f = [f_{21}, f_{31}, \cdots, f_{M1}]^{\mathrm{T}}, \tag{11}$$

$$\boldsymbol{Y} = [\boldsymbol{Y}_\tau \ \ \boldsymbol{Y}_f]^{\mathrm{T}} = h(\boldsymbol{u}). \tag{12}$$

The actual measured TDOA and FDOA have errors compared with the true value, which can be expressed as

$$\dot{\boldsymbol{Y}} = [\dot{\boldsymbol{Y}}_\tau \ \dot{\boldsymbol{Y}}_f]^{\mathrm{T}} = [\dot{\tau}_{21}, \dot{\tau}_{31}, \cdots, \dot{\tau}_{M1}, \dot{f}_{21}, \dot{f}_{31}, \cdots, \dot{f}_{M1}]^{\mathrm{T}} = h(\boldsymbol{u}) + \boldsymbol{N} \tag{13}$$

where $\boldsymbol{N} = [\boldsymbol{N}_\tau \ \ \boldsymbol{N}_f]^{\mathrm{T}}$, assuming that $\boldsymbol{N}_\tau$ and $\boldsymbol{N}_f$ obey independent Gaussian distribution, the covariance matrices are as follows:

$$\boldsymbol{Q} = \begin{bmatrix} \boldsymbol{Q}_\tau & \boldsymbol{0} \\ \boldsymbol{0} & \boldsymbol{Q}_f \end{bmatrix},$$

$$\boldsymbol{Q}_\tau = 0.5\delta_t^2\left[\boldsymbol{I} + \boldsymbol{1}^{\mathrm{T}}\right],$$

$$\boldsymbol{Q}_f = 0.5\delta_f^2\left[\boldsymbol{I} + \boldsymbol{1}^{\mathrm{T}}\right],$$

where δ_τ^2 and δ_f^2 are the variances of TDOA and FDOA measurement error, respectively.

The parameter to be estimated is $\boldsymbol{u}$, the observation vector is $\dot{\boldsymbol{Y}}_\tau$, then its probability density function is $p\left(\dot{\boldsymbol{Y}}_\tau;\boldsymbol{u}\right)$, and the Fisher information matrix based on TDOA [32] is

$$\boldsymbol{J}_\tau = \mathrm{E}\left\{\left[\frac{\partial \ln p\left(\dot{\boldsymbol{Y}}_\tau;\boldsymbol{u}\right)}{\partial \boldsymbol{u}}\right]^2\right\} = -\mathrm{E}\left\{\frac{\partial^2 \ln p\left(\dot{\boldsymbol{Y}}_\tau;\boldsymbol{u}\right)}{\partial \|\boldsymbol{u}\|}\right\} = \left(\frac{\partial \boldsymbol{d}}{\partial \boldsymbol{u}^{\mathrm{T}}}\right)^{\mathrm{T}} \boldsymbol{Q}_r^{-1}\left(\frac{\partial \boldsymbol{d}}{\partial \boldsymbol{u}^{\mathrm{T}}}\right) \tag{14}$$

where $\boldsymbol{Q}_r$ is the covariance matrix of TDOA measurement error

$$\frac{\partial \boldsymbol{d}}{\partial \boldsymbol{u}^{\mathrm{T}}} = [\mu_{\boldsymbol{u},\boldsymbol{s}_2} - \mu_{\boldsymbol{u},\boldsymbol{s}_1}, \mu_{\boldsymbol{u},\boldsymbol{s}_3} - \mu_{\boldsymbol{u},\boldsymbol{s}_1}, \cdots, \mu_{\boldsymbol{u},\boldsymbol{s}_M} - \mu_{\boldsymbol{u},\boldsymbol{s}_1}]^{\mathrm{T}}. \tag{15}$$

(i) Stationary target

The Fisher information matrix based on FDOA is

$$\boldsymbol{J}_f = \left(\frac{\partial \dot{\boldsymbol{d}}}{\partial \boldsymbol{u}^{\mathrm{T}}}\right)^{\mathrm{T}} \boldsymbol{Q}_f^{-1}\left(\frac{\partial \dot{\boldsymbol{d}}}{\partial \boldsymbol{u}^{\mathrm{T}}}\right) \tag{16}$$

where $\boldsymbol{Q}_f$ is the distance change rate measurement error covariance matrix

$$\frac{\partial \dot{\boldsymbol{d}}}{\partial \boldsymbol{u}^{\mathrm{T}}} = \begin{bmatrix} \mu_{\boldsymbol{u},\boldsymbol{s}_2}\dot{d}_2/d_2 - \mu_{\boldsymbol{u},\boldsymbol{s}_1}\dot{d}_1/d_1 - \gamma_{\dot{\boldsymbol{s}}_2} + \gamma_{\dot{\boldsymbol{s}}_1} \\ \mu_{\boldsymbol{u},\boldsymbol{s}_3}\dot{d}_3/d_3 - \mu_{\boldsymbol{u},\boldsymbol{s}_1}\dot{d}_1/d_1 - \gamma_{\dot{\boldsymbol{s}}_3} + \gamma_{\dot{\boldsymbol{s}}_1} \\ \vdots \\ \mu_{\boldsymbol{u},\boldsymbol{s}_M}\dot{d}_M/d_M - \mu_{\boldsymbol{u},\boldsymbol{s}_1}\dot{d}_1/d_1 - \gamma_{\dot{\boldsymbol{s}}_M} + \gamma_{\dot{\boldsymbol{s}}_1} \end{bmatrix}^{\mathrm{T}} \tag{17}$$

where $\gamma_{\dot{\boldsymbol{s}}_2} = -\boldsymbol{s}_i/d_i \ (i = 1, 2, \cdots, M)$.

The Fisher information matrix based on hybrid TDOA/FDOA is

$$\boldsymbol{J} = \left(\frac{\partial \boldsymbol{q}}{\partial \boldsymbol{u}^{\mathrm{T}}}\right)^{\mathrm{T}} \boldsymbol{Q}^{-1}\left(\frac{\partial \boldsymbol{q}}{\partial \boldsymbol{u}^{\mathrm{T}}}\right) \tag{18}$$

where $\boldsymbol{q} = \left[\boldsymbol{d}^{\mathrm{T}}, \dot{\boldsymbol{d}}^{\mathrm{T}}\right]$, $\dfrac{\partial \boldsymbol{q}}{\partial \boldsymbol{u}^{\mathrm{T}}} = \left[\dfrac{\partial \boldsymbol{r}}{\partial \boldsymbol{u}^{\mathrm{T}}}, \dfrac{\partial \dot{\boldsymbol{r}}}{\partial \boldsymbol{u}^{\mathrm{T}}}\right]^{\mathrm{T}}$, $\boldsymbol{Q} = \mathrm{Diag}[\boldsymbol{Q}_r, \boldsymbol{Q}_f]$.

(ii) Moving target

When the target is in motion, the position and velocity of the target need to be estimated at the same time. At this time, the parameter to be estimated is $\boldsymbol{\theta}=[\boldsymbol{u}^{\mathrm{T}} \ \dot{\boldsymbol{u}}^{\mathrm{T}}]^{\mathrm{T}}$, and the Fisher information matrix based on the target position and velocity of FDOA [33] is

$$\boldsymbol{J}_f = \left(\frac{\partial \dot{\boldsymbol{d}}}{\partial \boldsymbol{\theta}^{\mathrm{T}}}\right)^{\mathrm{T}} \boldsymbol{Q}_f^{-1}\left(\frac{\partial \dot{\boldsymbol{d}}}{\partial \boldsymbol{\theta}^{\mathrm{T}}}\right) \tag{19}$$

where

$$\frac{\partial \dot{\boldsymbol{d}}}{\partial \boldsymbol{\theta}^{\mathrm{T}}} = \left[\frac{\partial \dot{\boldsymbol{d}}}{\partial \boldsymbol{u}^{\mathrm{T}}}, \ \frac{\partial \dot{\boldsymbol{d}}}{\partial \dot{\boldsymbol{u}}^{\mathrm{T}}}\right],$$

$$\frac{\partial \dot{\boldsymbol{d}}}{\partial \boldsymbol{u}^{\mathrm{T}}} = \begin{bmatrix} \mu_{\boldsymbol{u},\boldsymbol{s}_2}\dot{d}_2/d_2 - \mu_{\boldsymbol{u},\boldsymbol{s}_1}\dot{d}_1/d_1 - \gamma_{\dot{\boldsymbol{u}},\dot{\boldsymbol{s}}_2} + \gamma_{\dot{\boldsymbol{u}},\dot{\boldsymbol{s}}_1} \\ \mu_{\boldsymbol{u},\boldsymbol{s}_3}\dot{d}_3/d_3 - \mu_{\boldsymbol{u},\boldsymbol{s}_1}\dot{d}_1/d_1 - \gamma_{\dot{\boldsymbol{u}},\dot{\boldsymbol{s}}_3} + \gamma_{\dot{\boldsymbol{u}},\dot{\boldsymbol{s}}_1} \\ \vdots \\ \mu_{\boldsymbol{u},\boldsymbol{s}_M}\dot{d}_M/d_M - \mu_{\boldsymbol{u},\boldsymbol{s}_1}\dot{d}_1/d_1 - \gamma_{\dot{\boldsymbol{u}},\dot{\boldsymbol{s}}_M} + \gamma_{\dot{\boldsymbol{u}},\dot{\boldsymbol{s}}_1} \end{bmatrix}^{\mathrm{T}}, \tag{20}$$

$$\frac{\partial \dot{\boldsymbol{d}}}{\partial \dot{\boldsymbol{u}}^{\mathrm{T}}} = \frac{\partial \boldsymbol{d}}{\partial \boldsymbol{u}^{\mathrm{T}}}, \tag{21}$$

where $\gamma_{\dot{\boldsymbol{u}},\dot{\boldsymbol{s}}_i} = (\dot{\boldsymbol{u}} - \dot{\boldsymbol{s}}_i)/r_i \ (i = 1, 2, \cdots, M)$.

The Fisher information matrix of the target position and velocity based on the hybrid TDOA/FDOA is

$$\boldsymbol{J} = \left(\frac{\partial \boldsymbol{q}}{\partial \boldsymbol{\theta}^{\mathrm{T}}}\right)^{\mathrm{T}} \boldsymbol{Q}^{-1}\left(\frac{\partial \boldsymbol{q}}{\partial \boldsymbol{\theta}^{\mathrm{T}}}\right) \tag{22}$$

where $\dfrac{\partial \boldsymbol{q}}{\partial \boldsymbol{\theta}^{\mathrm{T}}} = \begin{bmatrix} \partial \boldsymbol{r} / \partial \boldsymbol{u}^{\mathrm{T}} & \partial \boldsymbol{r} / \partial \dot{\boldsymbol{u}}^{\mathrm{T}} \\ \partial \dot{\boldsymbol{r}} / \partial \boldsymbol{u}^{\mathrm{T}} & \partial \dot{\boldsymbol{r}} / \partial \dot{\boldsymbol{u}}^{\mathrm{T}} \end{bmatrix}$, $\partial \boldsymbol{r} / \partial \dot{\boldsymbol{u}}^{\mathrm{T}}$ is an all-zero matrix of $(M-1)\times 2$.

The objective function of the A-optimality is $\arg\min \mathrm{tr}(\boldsymbol{J}^{-1})$. Whether it is for a stationary target or a moving target, the core of its optimization is to solve the minimum trace value of the CRLB matrix at the next moment.

4.2 Track optimization based on A-optimization criterion

The optimal trajectory of the UAV is to make the UAV move towards the maximum value of the Fisher matrix determinant at the next moment. However, in practical applications, considering the maximum turning angle $\theta_{\max}$ and movement velocity of the UAV, the optimal configuration conditions for target positioning cannot be achieved in a short time. Therefore, at each track node, a fan-shaped area with an angle range of $2\theta_{\max}$ is given, and the fan-shaped area is equally divided into 20

angles, and all 20 angles of the fan-shaped area are traversed to filter out the minimum trace value of the CRLB matrix. The corresponding angle is the flying velocity direction of the UAV at the next moment. Fig. 5 is the schematic diagram of flight path planning for UAV swarm.

Step 1 Given the position coordinates $\boldsymbol{S}_k = [\boldsymbol{s}_1(k), \boldsymbol{s}_2(k), \cdots, \boldsymbol{s}_M(k)]^{\mathrm{T}}$ of each drone at time k, the TDOA positioning measurement value τ_k, the FDOA positioning measurement value f_k;

Step 2 Solve the error covariance matrix $\boldsymbol{Q}_k$ of hybrid positioning;

Step 3 Use the constrained weighted least squares (CWLS) algorithm to solve the real-time position and velocity of the target radiation source;

Step 4 Calculate the CRLB matrix and solve the objective function;

Step 5 Get the optimal angle of UAV flight at the next moment.

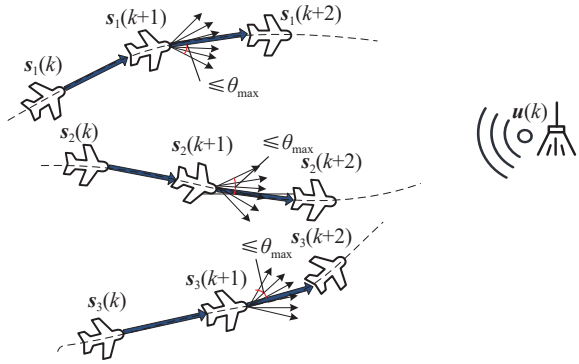

Fig. 5 Schematic diagram of flight path planning for UAV swarm

In summary, the data processing flow of UAV track planning based on A-optimality is shown in Fig. 6.

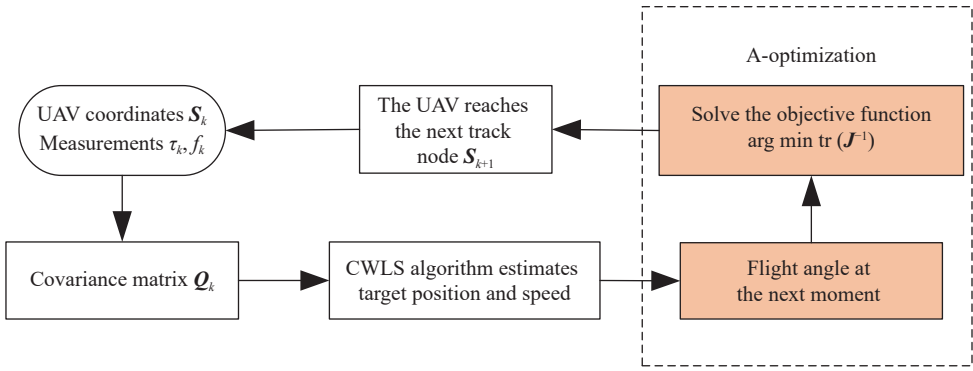

Fig. 6 Positioning and track planning process

5. Simulation

Suppose that four UAVs are used to locate the target. The initial state of the UAV is $\boldsymbol{s}_1(1) = [0, -8\,000, 0, -5\,000]^{\mathrm{T}}$, $\boldsymbol{s}_2(1) = [0, -7\,500, 0, -5\,000]^{\mathrm{T}}$, $\boldsymbol{s}_3(1) = [0, -7\,500, 0, -6\,000]^{\mathrm{T}}$, $\boldsymbol{s}_4(1) = [0, -7\,000, 0, -6\,000]^{\mathrm{T}}$, and all fly along the y axis at the initial moments, with a fixed flight velocity $v_u = 50$ m/s, maximum turning angle $\theta_{\max} = 10$, and sampling time interval $T = 1$ s, the signal-to-noise ratio SNR = 30 dB. The real position of the stationary target is $[0, 0, 0, 0]^{\mathrm{T}}$, and 100 Monte-Carlo simulations have been done, the following results are obtained.

5.1 Stationary target

Fig. 7(a) is the estimated distribution of the UAV swarm's optimized trajectory and target position to the stationary target. The approximate direction of motion of UAV2 and UAV3 is to fly toward the target, shortening the distance to the target, and UAV1 and UAV4 fly to both sides to form a better positioning configuration for estimating the target position, and the result of the target position estimation is gathered around the actual position. Fig.7(b) is the estimated distribution of the track and target position of the UAV swarm flying in a fixed configuration. When the UAV swarm flying in a fixed configuration, the distribution of the target position estimation results is relatively scattered. Fig. 7(c) shows the comparison of positioning error between optimized track and straight track, it is obvious that the error of the optimized track is lower than the error of the straight track, and the error of the optimized track starts to converge at about 16 s. A good positioning configuration is not formed, and the positioning error is slightly higher. On the straight track, the error generally shows a downward trend. This is because the distance between the UAV

swarm and the target is shortened, which improves the accuracy of positioning, but the positioning accuracy is not stable. This is because the relative configuration of positioning is very unfavorable for positioning the target.

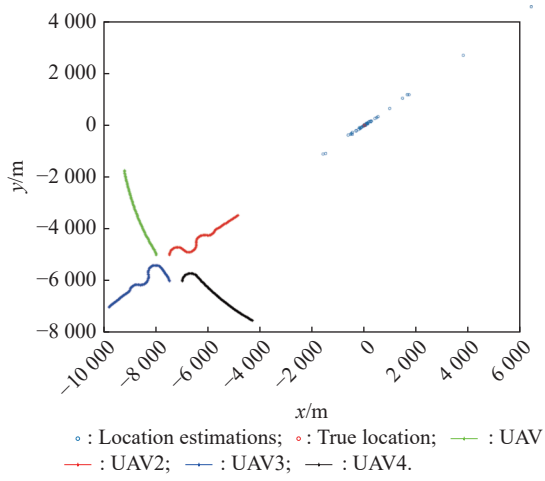

(a) Optimized track and target position estimation distribution

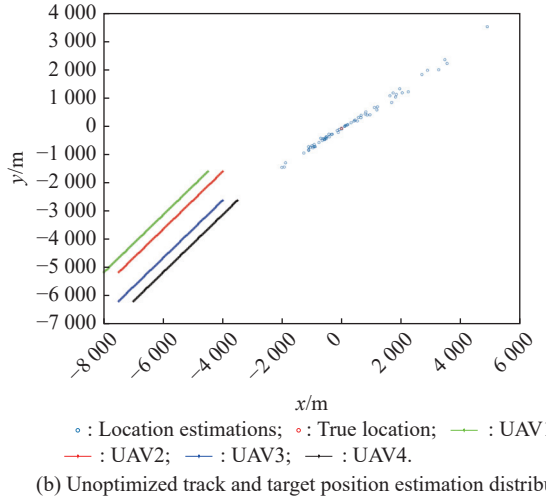

(b) Unoptimized track and target position estimation distribution

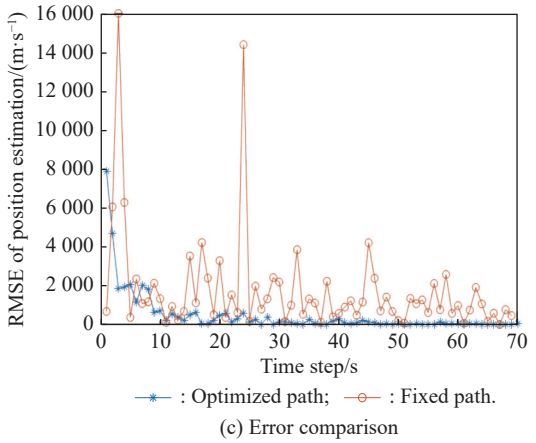

(c) Error comparison

Fig. 7 Position estimation result of stationary target

5.2 Moving target

The motion state of the target is divided into a uniform straight line and a uniform turning motion. The initial position is $[0,30\sqrt{2},0,30\sqrt{2}]^{\mathrm{T}}$, the uniform flight velocity of the target is $v_t = 30\sqrt{2}$ m/s, and the state transition matrix of the uniform turning is

$$F_k = \begin{bmatrix} 1 & \dfrac{\sin(\omega T)}{w} & 0 & -\dfrac{1-\cos(\omega T)}{\omega} \\ 0 & \cos(\omega T) & 0 & -\sin(\omega T) \\ 0 & \dfrac{1-\cos(\omega T)}{\omega} & 1 & \dfrac{\sin(\omega T)}{w} \\ 0 & \sin(\omega T) & 0 & \cos(\omega T) \end{bmatrix}$$

where $\omega = 0.1$.

5.2.1 Uniform linear motion

When the target is moving in a straight line at a constant velocity, the position of the target is constantly changing. At this time, the track optimization situation changes. The general trend of the UAV movement is to fly in all directions. From the distribution of the target position estimation results, the distribution of the positioning results after the optimization of track is more focused than that of the straight track. Fig. 8(c) also clearly reflects the positioning errors under the two tracks. The straight track has a higher positioning error for a uniform linear motion target. The positioning error of a stationary target is determined by the relative distance between the UAV swarm and the target. The shorter the distance, the higher the positioning accuracy. Fig. 8(d) is a comparison diagram of velocity estimation errors. It can be seen that the error of the optimized track is lower than that of the straight track.

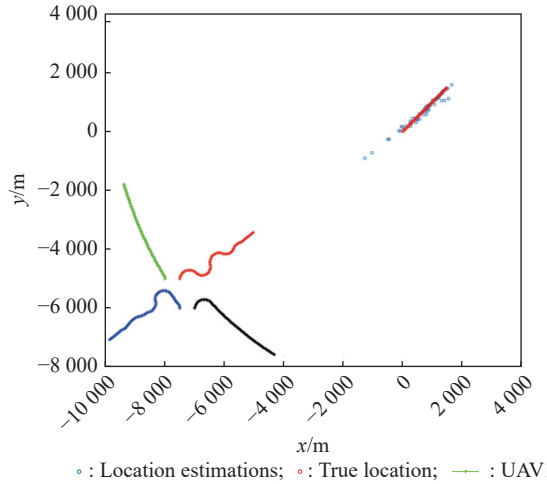

(a) Optimized track and target position estimation distribution

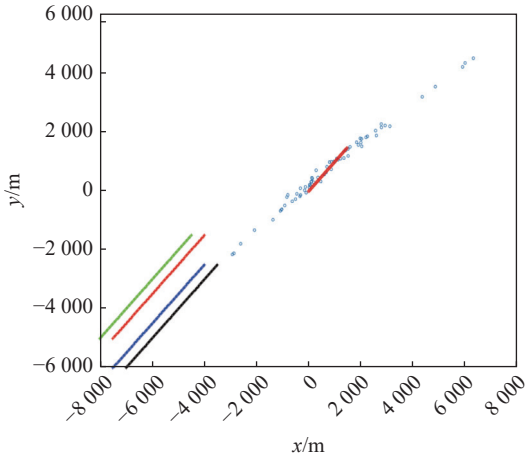

(b) Unoptimized track and target position estimation distribution

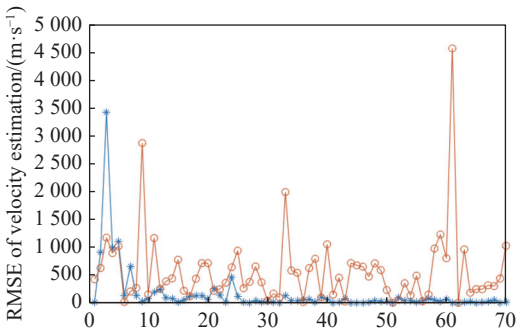

(c) Position estimation error comparison

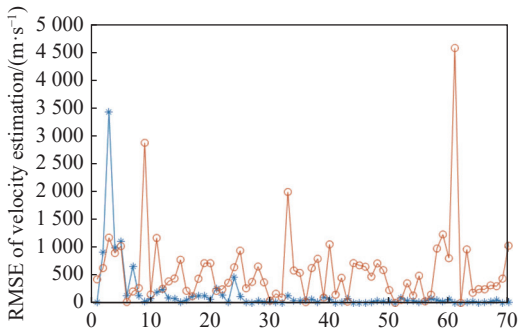

(d) Comparison of velocity estimation error

Fig. 8 Estimation results of the position and velocity of a uniformly moving target

5.2.2 Uniform turning motion

From Fig. 9, it can be found that when the target makes a uniform turning motion, it is more complicated than the first two motion modes. When optimizing the track, the overall trend of the UAV movement is also to fly in all directions, but it is also different from Fig. 7(a). At this time, the convergence velocity of the positioning error of the optimized track is lower than that of the first two motion modes, and it only converges in about 32 s. In a fixed configuration flight, the positioning accuracy of the target is not stable enough, and the fluctuations are large. Similarly, the velocity estimation error of the optimized track is also lower than that of the straight track.

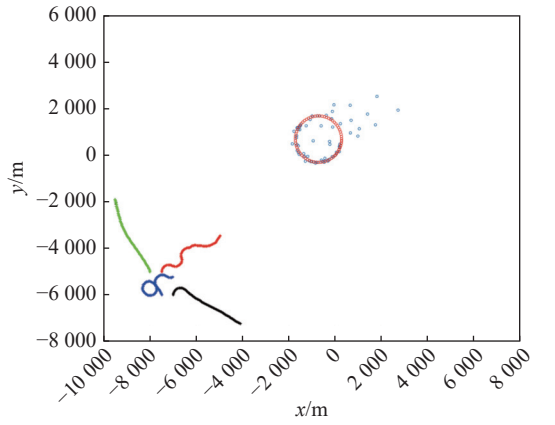

(a) Optimized track and target position estimation distribution

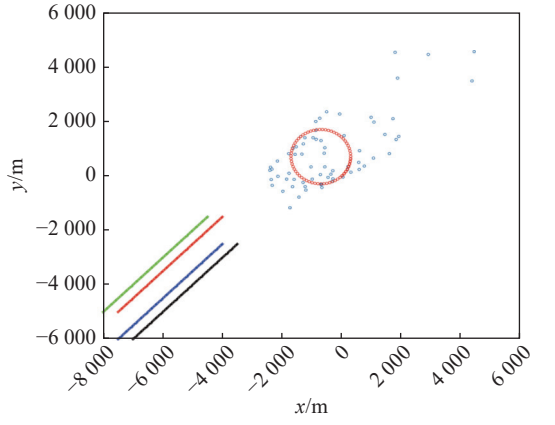

(b) Unoptimized track and target position estimation distribution

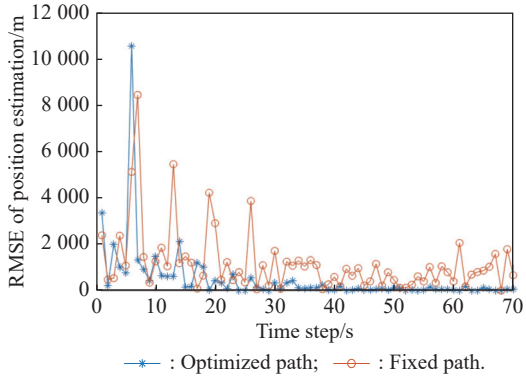

(c) Position estimation error comparison

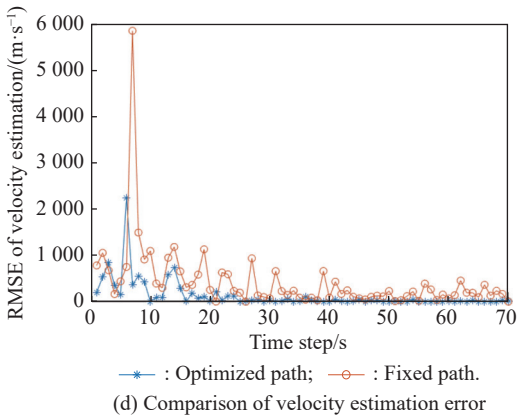

(d) Comparison of velocity estimation error

Fig. 9 Estimation results of position and velocity of moving target in uniform turning

6. Conclusions

In this paper, we establish a hybrid TDOA/FDOA positioning model, simulate and analyze the positioning accuracy of the model, theoretically derived the A-optimality criterion, and obtain the objective function of the UAV swarm hybrid TDOA/FDOA positioning track optimization. For stationary targets and moving targets, the simulation compares the position and velocity estimation errors of the optimized track and the straight track. Simulation analysis shows that for a stationary target, although the straight track can improve the positioning accuracy by shortening the relative distance to the target, it does not have convergence. The positioning error of the optimized track is adjusted after a period of configuration adjustment, it can converge to a lower level. For moving targets, the advantages of optimizing the track over the straight track are more obvious. Whether it is position estimation or speed estimation, linear tracks cannot achieve low error estimation, and optimized track improves the positioning accuracy of target positions and speeds by adjusting the positioning configuration in real time.

This paper considers the hybrid TDOA/FDOA positioning of the UAV swarm in a two-dimensional scene, and optimizes its track in real time. The next step will be extended to the three-dimensional scene and explore the real-time multi-step optimization of the track.

References

[1] GAO Y, LI D S, CHENG Z X. UAV distributed swarm situation awareness model. Journal of Electronics and Information Technology, 2018, 40(6): 1271–1278.

[2] LIANG X L, ZHANG J Q, LU N. UAV swarm. Xi'an: Northwestern Polytechnical University Press, 2018. (in Chinese)

[3] PHAM H X, LA H M, FEIL-SEIFER D, et al. Autonomous UAV navigation using reinforcement learning. https://doi.org/10.48550/arXiv.1801.05086.

[4] LIANG J. Geolocation-aware security in a netcentric small unmanned-aerial-system for RF emitters. Security and Communications Networks, 2015, 8(16): 2661–2670.

[5] SAPUTRA O D, IRFAN M, PUTRI N N, et al. UAV-based localization for distributed tactical wireless networks using archimedean spiral. Proc. of the International Symposium on Intelligent Signal Processing & Communication Systems, 2015. DOI: 10.1109/ispacs.2015.7432802.

[6] FOKIN G, ALI A. Algorithm for positioning in non-line-of-sight conditions using unmanned aerial vehicles. Proc. of the International Conference on Next-generation Teletraffic and Wired/wireless Advanced Networks and Systems, 2018. DOI: 10.1007/978-3-030-01168-0_44.

[7] ZHENG Y, SHENG M, LIU J Y, et al. Exploiting AoA estimation accuracy for indoor localization: a weighted AoA-based approach. IEEE Wireless Communications Letters, 2019, 8(1): 65–68.

[8] WANG Y, HO K C. An asymptotically efficient estimator in closed-form for 3-D AOA localization using a sensor network. IEEE Trans. on Wireless Communications, 2015, 14(12): 6524–6535.

[9] FOKIN G. AOA measurement processing for positioning using unmanned aerial vehicles. Proc. of the IEEE International Black Sea Conference on Communications and Networking, 2019. DOI: 10.1109/blackseacom.2019.8812834.

[10] TOMIC S, BEKO M, DINIS R. RSS-based localization in wireless sensor networks using convex relaxation: noncooperative and cooperative schemes. IEEE Trans. on Vehicular Technology, 2015, 64(5): 2037–2050.

[11] YANG S H, YUAN Z M, LI W, et al. Error data analytics on RSS range-based localization. Big Data Mining and Analytics, 2020, 3(3): 155–170.

[12] LIN L, SO H C, CHAN Y T. Accurate and simple source localization using differential received signal strength. Digital Signal Processing, 2013, 23(3): 736–743.

[13] WANG D, YIN J X, TANG T, et al. Quadratic constrained weighted least-squares method for TDOA source localization in the presence of clock synchronization bias: analysis and solution. Digital Signal Processing, 2018, 82(3): 237–257.

[14] HO K C, XU W. An accurate algebraic solution for moving source location using TDOA and FDOA measurements. IEEE Trans. on Signal Processing, 2004, 52(9): 2453–2463.

[15] YU H G, HUANG G M, GAO J, et al. Practical constrained least-square algorithm for moving source location using TDOA and FDOA measurements. Journal of Systems Engineering and Electronics, 2012, 23(4): 488–494.

[16] JIANG H Z, HU D X, ZHAO Y J, et al. A computationally efficient FDOA estimation method for radar pulse train. Proc. of the IEEE International Conference on Signal, Information and Data Processing, 2019. DOI: 10.1109/icsidp47821.2019.9173098.

[17] QUO F, HO K C. A quadratic constraint solution method for TDOA and FDOA localization. Proc. of the IEEE InternationalConferenceonAcoustics,2011.DOI: 10.1109/icassp.2011.5947014.

[18] LIU M Q, YI F, LIU P, et al. Cramer-Rao lower bounds of TDOA and FDOA estimation based on satellite signals. Proc. of the IEEE 14th International Conference on Signal Processing, 2018. DOI: 10.1109/icsp.2018.8652270.

[19] KIM D G, HAN J W, SONG K H, et al. Analysis of sensor-

emitter geometry for emitter localisation using TDOA and FDOA measurements. IET Radar, Sonar, and Navigation, 2017, 11(2): 341–349.
[20] TAKABAYASHI Y, MATSUZAKI T, KAMEDA H, et al. Target tracking using TDOA/FDOA measurements in the distributed sensor network. Proc. of the SICE Annual Conference, 2008. DOI: 10.1109/sice.2008.4655257.
[21] JAMSE P H, DAVID R M. Optimal observer trajectories for bearings-only tracking by minimizing the trace of the Cramer-Rao lower bound. Proc. of the 32th Conference on Decision and Control, 1993. DOI: 10.1109/cdc.1993.325008.
[22] FREW E W, DIXON C, ARGROW B, et al. Radio source localization by a cooperating UAV team. https://doi.org/10.2514/6.2005-6903.
[23] SEMPER S R, CRASSIDIS J L. Decentralized geolocation and optimal path planning using limited UAVs. Proc. of the 12th International Conference on Information Fusion, 2009. DOI: 10.1109/icuas.2015.7152274.
[24] CAO D B. Study on passive location and optimal observer trajectories for anti-radiation unmanned aerial vehicle. Changsha: National University of Defense Technology, 2010. (in Chinese)
[25] MORENO-SALINAS D, PASCOAL A, ARANDA J. Sensor networks for optimal target localization with bearings-only measurements in constrained three-dimensional scenarios. Sensors, 2013, 13(8): 10386–10417.
[26] HELFERTY J P, MUDGETT D R. Optimal observer trajectories for bearings only tracking by minimizing the trace of the Cramer-Rao lower bound. Proc. of the IEEE Conference on Decision and Control, 1993. DOI: 10.1109/cdc.1993.325008.
[27] OLSDER G J. On the optimal manoeuvering during bearings-only tracking. Proc. of the IEEE 23rd Conference on Decision and Control, 2007. DOI: 10.1109/cdc.1984.272153.
[28] YU H G, HUANG G M, GAO J, et al. Approximate maximum likelihood algorithm for moving source localization using TDOA and FDOA measurements. Chinese Journal of Aeronautics, 2012, 25(4): 593–597.
[29] LIU P T. An optimum approach in target tracking with bearing measurements. Journal of Optimization Theory & Applications, 1988, 56(2): 205–214.
[30] SHARP I, YU K. GDOP analysis for positioning design. Singapore: Springer, 2019.
[31] ALEXANDRAS A, TAFLANIDIS, JAMES L, et al. An efficient framework for optimal robust stochastic system design using stochastic simulation. Computer Methods in Applied Mechanics & Engineering, 2008, 198(1): 88–101.
[32] DOGANCAY D, HMAM H. On optimal sensor placement for time difference of arrival localization utilization uncertainty minimization. Proc. of the European Signal Processing Conference, 2009. DOI: 10.23919/eusipco.2017.8081442.
[33] MORENO-SALINAS D, PASCOAL A, ARANDA J. Optimal sensor placement for acoustic underwater target positioning with range-only measurements. IEEE Journal of Oceanic Engineering, 2016, 41(3): 620–643.

Biographies

LI Hao was born in 1981. He received his B.E. degree of radar engineering, and M.E. degree of information and communication engineering from Air Force Early Warning Academy, Wuhan, China. He received his Ph.D. degree in electronic science and technology from Air Force Engineering University in 2017, Xi'an, China. His research interests are swarm intelligence, UAV swarm, intelligence systems, and signal processing.
E-mail: afeu-li@163.com

SUN Hemin was born in 1972. He received his B.E. degree of radar engineering, and M.E. of degree weapon systems and applications from Air Force Early Warning Academy, Wuhan, China. His research interests are radar engineering and intelligence processing.
E-mail: skylar1013@126.com

ZHOU Ronghua was born in 1996. He received his B.E. degree of radar engineering from Air Force Early Warning Academy, Wuhan, China. He is pursuing his master degree in Air Force Early Warning Academy. His research interests are swarm intelligence, blind source separation, and intelligent optimization.
E-mail: 915216235@qq.com

ZHANG Huainian was born in 1984. He received his B.E. and M.E. degrees from the Second Artillery Command College, Wuhan, China. He is currently studying for his Ph.D. degree in information science at the Air Force Early Warning Academy, with a research direction of information fusion. His research interests are radar engineering and intelligence processing.
E-mail: 1241761040@qq.com